Наносистеми, наноматеріали, нанотехнології
Nanosistemi, Nanomateriali, Nanotehnologii
2026, т. 24, № 1, сс. 317–326
https://doi.org/10.15407/nnn.24.01.0317

PACS numbers: 64.75.Jk, 66.30.Pa, 68.37.Yz, 81.05.Bx, 81.16.Pr, 81.65.Kn, 81.65.Lp

Effect of Nanogold Layer on the Aluminizing Process of Superalloy BV-18 and Its Resistance to Hot Corrosion

M. M. Mahmood, M. A. Hamood, and S. M. Ahmed

Department of Physics,
The University of Mosul,
Mosul, Iraq

Nanolayer of gold is obtained by the method of physical vapour deposition as a thermal barrier on a nickel-base superalloy. The effect of this layer on the aluminizing process and the efficiency for hot-corrosion resistance is studied by comparing two sets of samples: the first set, which is contained of the gold layer, while the second set is aluminized without this layer. The aluminizing process is carried out for both sets, using the pack-cementation method at a temperature of 1000°C. The samples coated with nanogold show a different behaviour from those samples, which are aluminized only, where the use of nanogold oxide improves the alloy ability to withstand hot-corrosion conditions.

Наношар золота було одержано методом фізичного осадження з парової фази як тепловий бар'єр на ніклевому суперстопі. Вплив цього шару на процес алюмінування й ефективність стійкости до гарячої корозії було досліджено шляхом порівняння двох наборів зразків: перший набір містив шар золота, а другий набір був алюмінований без цього шару. Процес алюмінування проводився для обох наборів методом пакувальної цементації за температури у 1000°C. Зразки, покриті нанозолотом, демонстрували іншу поведінку, ніж ті, що були лише алюміновані, де використання нанооксиду Ауруму поліпшило здатність стопу витримувати умови гарячої корозії.

Key words: diffusion coating, hot corrosion, nanogold, pack cementation, surface engineering.

Ключові слова: дифузійне покриття, гаряча корозія, нанозолото, тверда цементація, інженерія поверхні.

(Received 26 August, 2024; in revised form, 8 September, 2024)

1. INTRODUCTION

Diffusion coatings were developed firstly and are used primarily to enrich the surface of the superalloy with aluminium. These coatings proved very successful and in the early to mid-1960s, this coating technique was applied to turbine blades made of nickel alloys [1–3]. There are a number of methods of forming aluminide coatings such as slurry spraying followed by high temperature diffusion, electrolysis and pack cementation. Of all these methods, pack cementation is the one widely used, as it is inexpensive and ideally suited for coating small components [4–6]. Despite the mentioned features, the diffusion of Ni from the superalloy and that of Al from the overlay causes, however, structural changes capable of causing spall off of the protecting layer [7]. Diffusion barrier coating systems have excellent mechanical properties (creep and fatigue), improving alloy substrate performance, and enhance the anti-exfoliation properties of YSZ in thermal barrier coatings (TBC) in addition to providing excellent oxidation resistance [8]. Adding a layer of yttrium oxide (Y_2O_3) to the alloy Fe–30 Cr before the aluminizing process improves its resistance to oxidation, as the yttrium oxide layer acts as a diffusion barrier that prevents the spread of aluminium from the coating layer into the alloy and preventing the spread of the alloy elements outward. The concentration of the element yttrium has an effect on the properties of the coating resulting from the aluminizing process, small amounts of it act as nucleation sites that impede the growth of granules, while adding large amounts of it leads to delaying the phase transformation $\theta\text{-}Al_2O_3 \rightarrow \alpha\text{-}Al_2O_3$ [9]. The diffusion barrier may partially prevent the interdiffusion of the alloy elements, thus improving the oxidation resistance of thermal barrier coatings (TBCs), where the content of aluminium and chromium was higher, while the rest of the alloy elements were lower in the mixture coating material for the sample with the diffusion barrier compared to the one without the barrier [10]. In this research, adding a nanogold layer as a thermal barrier to a nickel-based alloy and study the effect of that layer on the aluminizing process and efficiency of hot corrosion for the BV-18 nickel-based superalloy. The resulting coatings were analysed quantitatively and qualitatively for both types of coating using x-ray spectroscopy (XRD), (SEM), and (EDX) techniques to determine the compounds that make up the coating and their phases.

2. EXPERIMENTAL METHODS

2.1. Materials

In this study, the superalloy BV-18 is used, which is one of the

blades of turbine engines used in gas stations to generate electrical power; its quantitative and qualitative specifications are shown in Table 1.

2.2. Coating Processes

In this study, two types of coating techniques are used.

2.2.1. Pack Cementation

Aluminizing is performed in a tube furnace under vacuum, which is maintained throughout the process (heating, holding, and cooling).

The cementation process was carried out for all prepared samples and for the superalloy BV-18 using a mixture of aluminium powder 30% as the coating material, aluminium oxide (alumina) 66% as a material that helps prevent agglomeration of the mixture, and ammonium chloride powder. With a percentage of 4% as an activating material, the mixture is placed after good mixing inside the pod gradually, while placing the samples to be coated in it. The pod is closed and placed inside a vacuum oven according to Fig. 1.

The temperature of the oven is set at the required degree 1000°C. Cementing takes place for a period of 6 hours, and after the completion of the coating process, the samples are cooled inside the oven until the temperature (of 200°C) reaches, while continuing to operate the vacuum device. Then, the samples are taken out, cleaned, then weighed and stored well until tests are conducted on them.

TABLE 1. Composition [wt.%] of superalloy BV-18 used in the experiments.

Element	Ni	Cr	Ti	Co	Mo	Al	C	Si	S
wt.%	balance	17.85	4.15	5.31	2.28	10.53	8.79	4.99	3.57

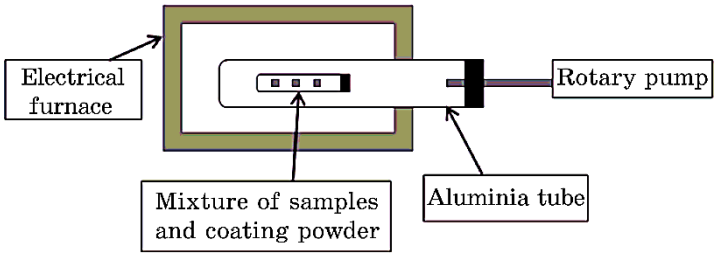

Fig. 1. Schematic drawing of the coating system.

Fig. 2. Q150R ES device used to deposit nanogold layer.

TABLE 2. Composition [wt.%] of the coated superalloy BV-18.

Type of coating	Element	Al	Ni	Co	Cr	Au	Si	Mo
Single aluminizing	wt.%	21.21	25.52	16.08	8.18	Non	0.42	0.66
Nanogold	wt.%	24.00	12.62	3.01	2.32	1.99	0.76	0.00

2.2.2. Nanogold Layer Coating

There are different techniques for fixing the diffusion barrier material on the surface of the sample, including chemical evaporation (CVD) or physical (PVD) coating, laser coating, and others. In this study, the sputtering coating technique was used. This method is one of the physical evaporation (PVD) methods and is a widely used technique. To deposit thin films, a nanogold layer was deposited on some samples of the alloy BV-18 targeted in our study using a device (Q150R ES), the image of which is shown in Fig. 2. Sputter target/disc style 57 mm×0.1 mm thick gold.

3. RESULTS AND DISCUSSION

3.1. Surface Morphology

The results were obtained after aluminizing the superalloy BV-18 with pack-cementation process through a single aluminizing process and aluminizing in the presence of the nanogold at a temperature of 1000°C and for time period of 6 h. For each processing mode, single set of parameter was used: high temperature with high Al activity (HTHA).

The results of the analysis of the scanning electron microscopy (SEM) shown in Fig. 3 for the two types of coatings showed a homogeneous spread of aluminium.

From spectroscopic analysis of the EDS (Figs. 4, 5), there are

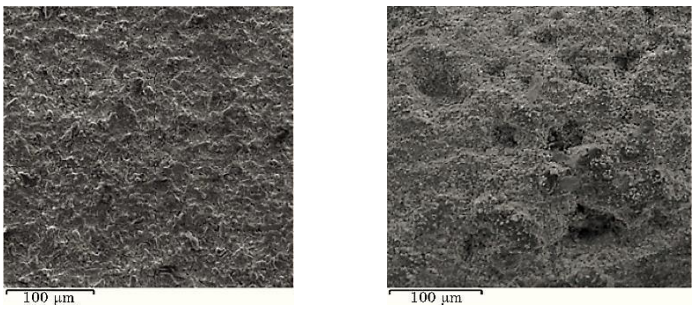

a *b*

Fig. 3. Surface morphology of aluminizing with: *a*—single aluminizing; *b*—nanogold.

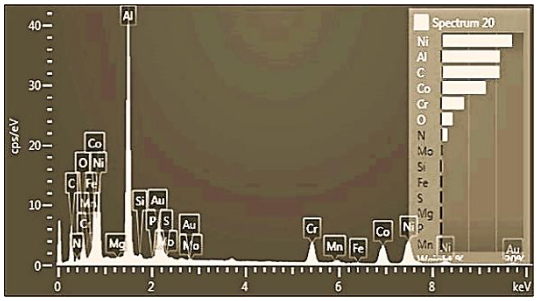

Fig. 4. EDS for aluminizing coating for single aluminizing of BV-18 superalloy at 1000°C for 6 h.

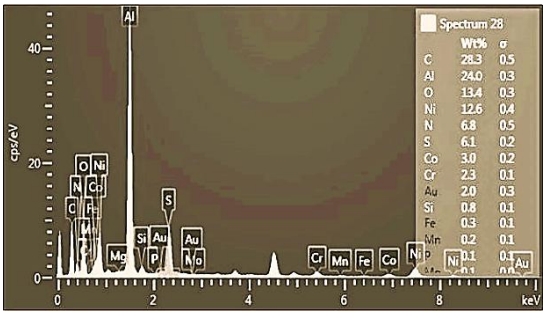

Fig. 5. EDS for aluminizing coating in the presence of nanogold layer for BV-18 superalloy at 1000°C for 6 h.

many peaks for the elements, including aluminium, nickel and cobalt, and the highest intensity of these peaks is the element aluminium, which represents the basic element for the coating layer.

This is what appeared in the data of Table 3 for quantitative and

TABLE 3. Average mass gain and average thickness of aluminized samples by single aluminizing and nanogold for BV-18 superalloy for 6 h at 1000°C.

Type of coating	Av. thickness of coating, μm	Mass gain, mg/cm^2
Single aluminizing	350	48.63
Nanogold	358	40.57

TABLE 4. The phases are possible to form in single aluminizing coating.

Ref. Code	Compound Name	Chemical Formula
03-065-0672	Aluminium Cobalt	AlCo
00-002-1261	Aluminium Nickel	AlNi
00-002-1239	Aluminium Chromium	$AlCr_2$
00-021-0008	Aluminium Nickel	$AlNi_3$
00-038-1026	Aluminium Chromium	$Al_{86}Cr_{14}$
03-065-3454	Aluminium Nickel	Al_3Ni_2
03-065-7336	Aluminium Chromium	$Al_{0.983}Cr_{0.017}$
03-065-8530	Aluminium Molybdenum	$AlMo_3$
00-042-1467	Cobalt Oxide	Co_3O_4
00-032-0285	Chromium Oxide	CrO_3

TABLE 5. The phases are possible to form in aluminizing process in presence of nanogold layer.

Ref. Code	Compound Name	Chemical Formula
03-065-8473	Aluminium Gold	Al_2Au
01-075-1865	Aluminium Oxide	Al_2O_3
00-029-0021	Aluminium Cobalt	AlCo
00-002-1261	Aluminium Nickel	AlNi
00-047-1410	Aluminium Titanium	$AlTi_2$
01-089-3697	Gold	Au

qualitative analysis by the scanning electron device (EDS).

The percentage of aluminium and nickel is shown in Table 5. This supports the analysis of XRD spectrum in obtaining the intermediate compounds of nickel–aluminium, as well as obtaining some intermediate compounds of cobalt–aluminium, with a weight ratio [wt.%] of cobalt.

3.2. Optical Microscopy Examination

The samples that were coated with single aluminium using the pack-

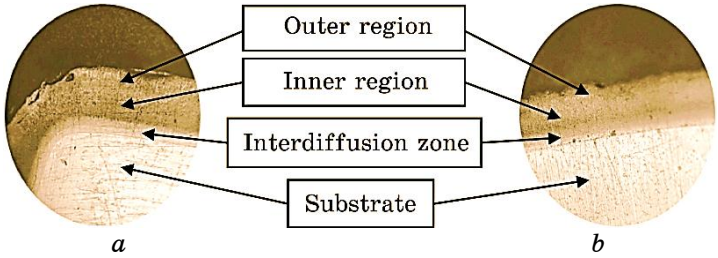

Fig. 6. Microstructure of the samples coated with two types of aluminizing coatings: (*a*) single aluminizing; (*b*) nanogold at temperature of 1000°C for 6 h.

cementations method showed the appearance of three areas of coating: the outer layer, the inner region and, interdiffusion zone, which is a narrow area free of deposits. The cross-section of the samples was photographed as shown in Fig. 6 for two types of coatings (*a*—single aluminizing; *b*—nanogold). The thickness of coating with single aluminizing and nanogold with mass gain value are shown in Table 3.

The microscopic examination of the coating after 6 h showed the presence of two regions, the outer region containing dark structures, which may be secondary phases, and the inner region having light-coloured structures, somewhat narrow and a little thick at the bottom, *i.e.*, the interdiffusion zone. This is known as the diffusive exchange zone. It is also noted that the microscopic structure of the resulting coatings is characterized by the presence of more than one phase in the coating layer, and the outer coating layer consists of phases rich in aluminium.

3.3. XRD Analysis

It must be remembered that the alloy used in the research is nickel-based, and its coating with aluminium leads to the formation of one of the phases of intermediate compounds nickel–aluminium, and this has already happened. The results of XRD analysis revealed many complications in terms of the number of resulting phases, but they confirmed the formation of the aluminium-rich phase Ni–Al and Ni_2Al_3 are mainly in the coatings produced after 6 hours this is consistent with what was stated in Ref. [11] for high temperature–high activity aluminize coating.

The results of the x-ray diffraction analysis of the coated sample for a period of 6 hours, as was shown from the diffraction model in Fig. 7, the appearance of peaks by returning to the phase diagrams for both systems nickel–aluminium and aluminium–gold. In Figures

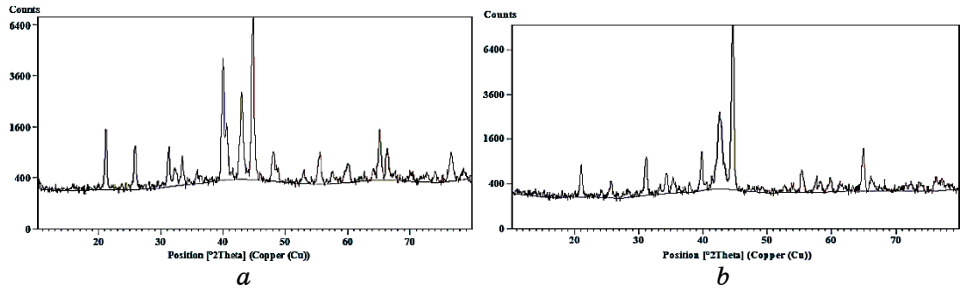

Fig. 7. X-ray diffraction plot of a sample coated with: (*a*) single aluminizing; (*b*) nanogold at 1000°C for 6 hours.

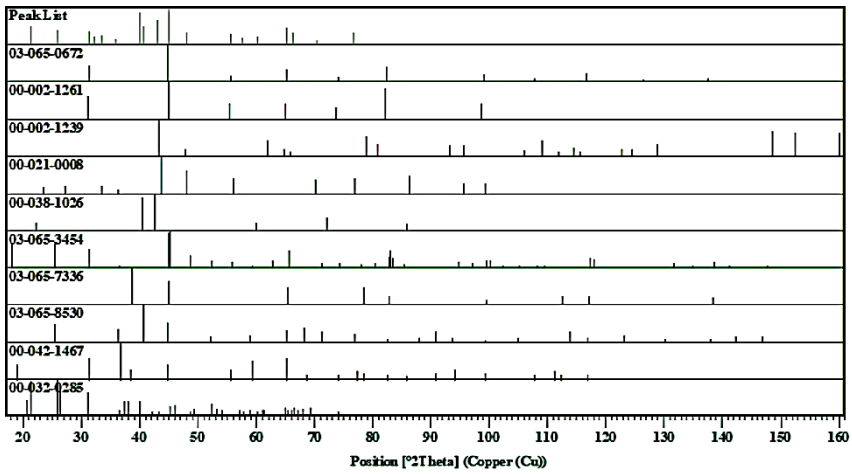

Fig. 8. Comparison of the results of X-ray analysis that are formed in a single aluminizing coating for BV-18 superalloy at 1000°C for 6 h with those stored in the X'Pert High Score Plus program.

8 and 9, we find that the phases are possible to form at this temperature. Tables 4 and 5 show the phases, which are possible to form in single aluminizing and with nanogold layer.

3.4. Hot-Corrosion Test

This test was conducted with the aim of identifying the resistance of the single aluminized sample compared to the aluminized sample in presence of nanogold layer for hot corrosion conditions, and the test results have been shown by studying (the change of mass with time) in salt vapour at 900°C. As shown in Fig. 10, the sample aluminized with single aluminizing suffered some decreasing in mass in the first

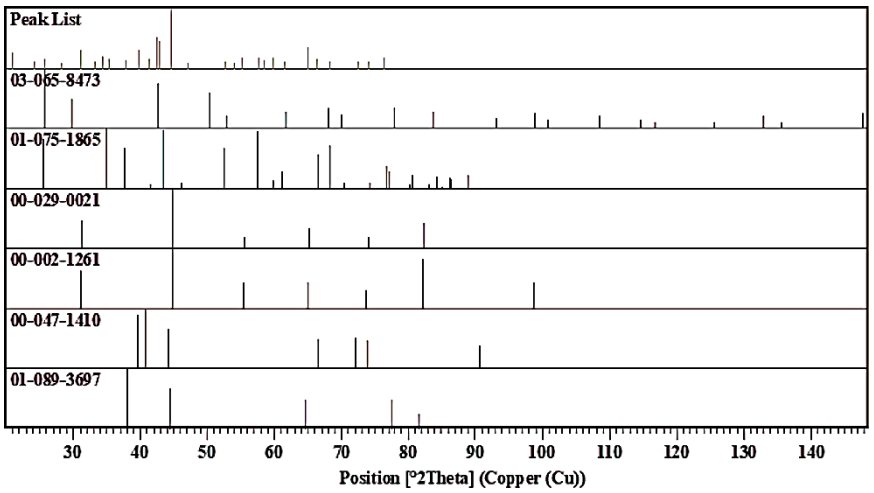

Fig. 9. Comparison of the results of x-ray analysis, which are obtained for the aluminizing coating in the presence of nanogold layer for BV-18 superalloy at 1000°C for 6 h, with those stored in the X'Pert High Score Plus program.

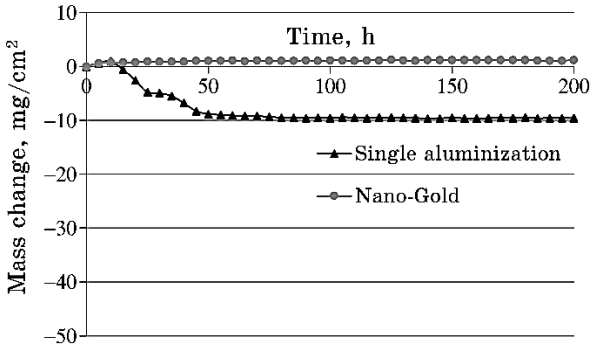

Fig. 10. Cyclic oxidation kinetics of single aluminizing coating and in presence of nanogold layer in salt vapour at 900°C.

50 hours of exposure, while stability in mass was observed with alloy that coated with nanogold layer before aluminizing process.

4. CONCLUSIONS

In this research, the effect of adding nanogold layer as a thermal barrier on (aluminizing process and resisting hot corrosion) was studied. It is indicated from the (Microscopic, XRD, SEM-EDS) analysis that inward diffusion of Al and outward diffusion of Co,

Ni and Cr have led to the formation of multilayer with different phases, the addition of nanogold produce some different phases such as Al_2Au and stable alumina phase (Ref. Code 01-075-1865), namely, α-Al_2O_3. By monitoring the weight loss and the data obtained from the kinetics of oxidation, it was shown that the coating in the presence of nanogold has the best resistance to hot corrosion and had less change in mass during the test compared to single aluminized, and the protective oxidation scale α-Al_2O_3 has very good adhesion and stability during exposure time. Overall, for the above, this thermal barrier is considered with a high efficiency in resisting the harsh operating conditions of engineering equipment.

ACKNOWLEDGMENTS

We would like to express our heartfelt gratitude to the University of Mosul/College of Science and to Dr. Mohammad M. Uonis (Department of Physics, College of Science, Mosul University, Mosul, Iraq), for their unwavering assistance throughout the research process.

REFERENCES

1. S. Bose, *High Temperature Coatings* (Elsevier Science: 2017).
2. G. W. Goward and L. W. Cannon, *J. Eng. Gas Turbines Power*, **110**, Iss. 1: 150 (1988); https://doi:10.1115/1.3240078
3. J. R. Nicholls, *JOM*, **52**, Iss. 1: 28 (2000); https://doi:10.1007/s11837-000-0112-2
4. R. Sivakumar and B. L. Mordike, *Surface and Coating Technology*, **37**, Iss. 2: 139 (1989).
5. M. O. Cojocaru, M. Branzei, and L. N. Druga, *Materials*, **15**, Iss. 15: 5453 (2022); https://doi:10.3390/ma15155453
6. R. Bianco and R. A. Rapp, *Pack Cementation Diffusion Coatings BT–Metallurgical and Ceramic Protective Coatings* (Ed. K. H. Stern) (Netherlands: Springer: 1996), p. 236; https://doi:10.1007/978-94-009-1501-5_9
7. M. Uunonen, P. Kaski, P. Henttu, and P. Kettunen, *Diffusion Barriers for the Superalloy Blades of Gas Turbines- Steels and Materials for Power Plants* (Eds. P. Neumann, D. Allen, and E. Teuckhoff) (Weinheim: Wiley-VCH: 2000), p. 332; https://doi.org/10.1002/3527606181.ch58
8. T. Narita, Y. Kato, T. Narita, and M. Ara, *High Temp. Corros. Mater.*, **100**, Iss. 5: 399 (2023); https://doi:10.1007/s11085-023-10203-0
9. C. Houngninou, S. Chevalier, and J. P. Larpin, *Appl. Surf. Sci.*, **236**, Iss. 1: 256 (2004); https://doi.org/10.1016/j.apsusc.2004.04.026
10. Z. Xu, L. He, R. Mu, X. Zhong, and X. Cao, *Vacuum*, **82**, Iss. 11: 1251 (2008); https://doi.org/10.1016/j.vacuum.2008.03.057
11. E. Pauletti and A. S. C. M. d'Oliveira, *J. Vac. Sci. Technol. A*, **36**, Iss. 4: 41504 (2018); https://doi:10.1116/1.5026272